While earlier preliminary time–resolved fluorescence experiments [19] on **C_{60}[11]DMA**, in which the DMA chromophore was excited, indicated that the UV emission emerging from this chromophore is strongly quenched by energy (or electron) transfer, the fluorescence decays now observed for the red emission at 707 nm of the fullerene, using single photon counting in methylcyclohexane give a fluorescence lifetime of 1344 ± 10 ps for both **C_{60}[11]DMA** and **C_{60}[11]**. In the polar solvent benzonitrile, in which both luminescence and population of the triplet state for **C_{60}[11]DMA** are strongly quenched, fluorescence decay from the fullerene unit displays a major fast component of 160 ± 10 ps.

The rate of charge separation for **C_{60}[11]DMA** in benzonitrile is estimated from eqn (2) to be k_{cs} = 5.5 x 10^9 s^{-1}:

$$k_{cs} = 1/\tau - 1/\tau_{ref} \qquad (2)$$

In this equation, the lifetime of **C_{60}[11]DMA** (or **C_{60}[11]**) in methylcyclohexane is taken to be equal to τ_{ref}. Application of eqn (1) to the quantum yield data from Table 5.2 gives the quite similar value for k_{cs}: 5.1 x 10^9 s^{-1}.

From these data the quantum yield for charge separation *via* the excited singlet state of the fullerene unit is estimated to be $k_{cs}/[1/\tau_{ref} + k_{cs}]$x100 = 87 to 88 %, which is in excellent agreement with the estimate made from the transient absorption spectra.

In order to determine the barrier for electron transfer experimentally, the temperature dependence of the fluorescence quantum yield of **C_{60}[11]DMA** in benzonitrile was investigated (see Table 5.3 for primary data).

Table 5.3. *Primary data used for the determination of the barrier to charge separation for* **C_{60}[11]DMA** *in benzonitrile: the relative emission yield* (Φ_{rel}) *at temperature (T) together with the rate of electron transfer obtained via formula (1).*

T (K)	Φ_{rel}	k_{cs}(s^{-1}))
295	1	4.74 x 10^9
290	1.05	4.47 x 10^9
285	1.09	4.27 x 10^9
280	1.14	4.04 x 10^9
275	1.20	3.82 x 10^9
270	1.26	3.59 x 10^9
265	1.34	3.33 x 10^9

As a reference, **C_{60}[11]** was employed, for which the fluorescence quantum yield is virtually temperature independent. From these measurements, electron transfer rates were derived *via* eqn (1). Linear regression for a plot (see Figure 5.4) of the natural logarithm of the electron

transfer rates multiplied by the square root of T, as a function of 1/T, leads to an intercept of 28.64 (= ln k_{opt} ($s^{-1}K^{0.5}$)), and a slope of 1038.1 (= $\Delta G^{\#} / k_B$ (K)). The barrier of electron transfer is therefore determined [20] to be $\Delta G^{\#} = 0.09$ eV.

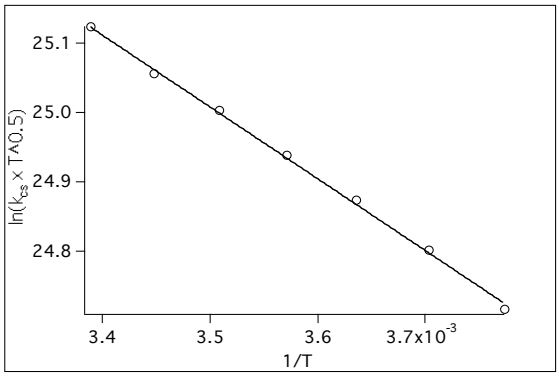

Fig. 5.4. *Modified [20] Arrhenius plot* $ln(k_{cs} \times \sqrt{T}) = ln(k_{opt}) - (\Delta G^{\#} / k_B) \times 1/T$ *for* **C_{60}[11]DMA** *obtained in benzonitrile.*

The conformation of the adduct **C_{60}[11]DMA** obtained by energy minimization [21] with semi-empirical AM1 calculations is shown in Figure 5.5. The center–to–center distance between the two chromophores is estimated to be *ca.* 18 Å, the edge–to–edge distance is *ca.* 12.6 Å.

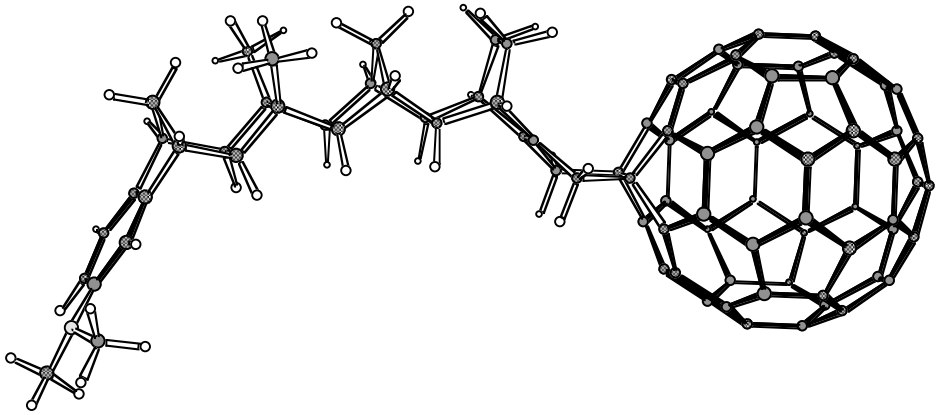

Fig. 5.5. *Structure of* **C_{60}[11]DMA** *obtained with AM1.*

With these geometrical data in hand, together with the electrochemical and photophysical data for the constituent chromophores, the barrier to photoinduced electron transfer can also be predicted, in principle, from the Marcus equation (3):

$$\Delta G_{cs}^{\#} = (\Delta G_{cs} + \lambda)^2 / 4\lambda \qquad (3)$$

Here, ΔG_{cs} is the Gibbs free energy change and λ the total reorganization energy. The former can be approximated as proposed by Weller *et al.* [22] *via*:

$$\Delta G_{cs} = e(E^{ox}(D) - E^{red}(A)) - E_{00} - e^2/4\pi\varepsilon_o\,\varepsilon_s R_c - e^2/8\pi\varepsilon_o\,(1/r^+ + 1/r^-)(1/37.5 - 1/\varepsilon_s) \qquad (4)$$

Calculation of ΔG_{cs} from eqn. (4) requires, in addition to the donor and acceptor redox potentials (+ 0.71 V and -0.57 V *vs* SCE) and the singlet or triplet state energy ($^1E_{00}$ = 1.76 eV and $^3E_{00}$ = 1.50 eV) [7a], knowledge of the center–to–center distance (R_c) and the effective ionic radii of the donor and acceptor radical cation and anion (r^+, respectively r^-). A value of 18 Å was estimated for R_c from our modeling results (Figure 5.5). Values for r^+ and r^- were calculated from the apparent molar volumes of *N,N*-dimethylaniline (density = ρ = 0.956) and of C_{60} (density 1.65), using a spherical approach.

$$4/3\ \pi\ r^3 = M/N\rho \qquad (5)$$

Here, M is the molecular weight and N is Avogadro's number. This gives r^+ = 3.7 Å and r^- = 5.6 Å. The calculated ΔG_{cs} values in various solvents are listed in Table 5.4 for both singlet and triplet charge separation.

The reorganization energy λ may be partitioned into internal (λ_i) and solvent (λ_s) contributions. The internal reorganization energy was set at λ_i = 0.3 eV [7a], while λ_s was calculated [13] using the Born-Hush approach (eqn (6)):

$$\lambda_s = e^2/4\pi\varepsilon_o\,(1/r - 1/R_c)(1/n^2 - 1/\varepsilon_s) \qquad (6)$$

In agreement with the fluorescence data discussed above it is found that the driving force for charge separation ($-\Delta G_{cs}$) from the fullerene S_1 state becomes positive in solvents more polar than diethyl ether [23]. Furthermore the calculated barrier (0.11 eV) for electron transfer in benzonitrile is in reasonable agreement with the experimental value (0.09 eV). As we have shown earlier [20a], this agreement as well as the high linearity of the Arrhenius plot obtained (see Figure 5.4) are typical for electron transfer processes taking place in the 'normal' Marcus region if performed in polar media.

It is important to note that, due to the relatively small S_1-T_1 energy gap of the fullerene chromophore, photoinduced charge separation from the T_1 state can also become exergonic in sufficiently polar media such as benzonitrile (see Table 5.4). As discussed above however, charge separation from the S_1 state is so rapid in this solvent that it accounts for *ca.* 90% of

the fullerene's S_1 decay modes, thereby overwhelming the otherwise efficient intersystem crossing of the fullerene chromophore (k_{isc} ~ 7.5 x 10^8 s^{-1}).

Table 5.4. *Reorganization energy ($\lambda = \lambda_s$ + 0.3 eV), Gibbs free energy change (ΔG_{cs}), and barrier ($\Delta G_{cs}^{\#}$) for charge separation in various solvents (dielectric constant* ε, *refractive index* n*) from both the singlet and triplet (T) state, of the fullerene chromophore in* **C_{60}[11]DMA**, *as calculated via eqns. (3), (4) and (6).*

				Charge separation from singlet state		Charge separation from triplet state	
solvent	ε	n	λ (eV)	ΔG_{cs} (eV)	$\Delta G_{cs}^{\#}$ (eV)	ΔG_{cs}(T) (eV)	$\Delta G_{cs}^{\#}$(T) (eV)
methylcyclohexane	2.07	1.423	0.33	0.61	0.58	0.87	1.09
1,4-dioxane	2.209	1.422	0.36	0.53	0.40	0.79	0.80
toluene	2.38	1.497	0.40	0.50	0.48	0.72	0.35
diethyl ether	4.20	1.35	1.01	0.01	0.25	0.27	0.28
1,2-dichlorobenzene	9.93	1.552	1.02	-0.32	0.12	-0.06	0.23
benzonitrile	25.20	1.528	1.20	-0.47	0.11	-0.21	0.20

5.4 Evaluation of the electronic coupling in C_{60}[11]DMA

The high rates of charge separation and recombination in **C_{60}[3]DMA** and **C_{60}[3]TMPD** are not surprising in view of the fact that bridges with an effective length of three sigma bonds are known to provide quite strong through–bond and though–space electronic coupling between the D and A units, which may even be sufficiently strong to bring the electron transfer processes into the adiabatic regime.

The high rate of photoinduced charge separation, as opposed to the relatively slow recombination in **C_{60}[11]DMA** is surprising because both the calculated and experimentally determined barrier to charge separation (0.11 and 0.09 eV, respectively) is significantly higher than in systems for which we have previously observed fast photoinduced charge separation across bridges of similar length [13]. It is therefore interesting to compare the electronic coupling matrix element (V^*) involved in the excited state charge separation process for **C_{60}[11]DMA** with that determined earlier for other bridged systems. This can be done readily using the non-adiabatic expression for electron transfer processes [20a] given by eqn. (7):

$$k_{cs} = \frac{2\pi^{3/2}}{h\sqrt{\lambda k_B T}}(V^*)^2 \exp\left[\frac{-\Delta G_{cs}^{\#}}{k_B T}\right] \quad (7)$$

Substitution of k_{cs}(5.5 x 10^9 s^{-1} at 300 K), and $\Delta G_{cs}^{\#}$ (0.09 eV), together with an estimated total reorganization energy of 1.2 eV (see Table 5.4), leads to V^* = 28 cm^{-1} [24]. Table 5.5 presents a compilation of values of coupling matrix elements for excited state electron transfer (V^*) and for thermal electron transfer (V) in a variety of donor–bridge–acceptor systems possessing effective bridge lengths ranging from four to ten sigma bonds. In Figure 5.6, the V and V^* values are plotted semilogarithmically against the number, n, of sigma bonds in the bridge for each series of systems. The plots display the expected (approximate) exponential decay of V and V^* with bridge length (n).

In spite the fact that the data compiled in Table 5.6 refer to a variety of bridges and D/A chromophores, it is evident that the V^* value of *ca.* 28 cm^{-1} derived for **C_{60}[11]DMA** is exceptionally large, and in fact exceeds the expected value for an 11-bond bridge by about an order of magnitude. The only report of similarly large V values refers to the work of Penfield *et al.* [27], who measured the inter valence absorption bands in the anion radicals of the **DMN[*n*]DCV** series of molecules (Table 5.5), arising from through-bond electronic coupling between the 1,1–dicyanovinyl (DCV) radical anion and the 1,4–dimethoxynaphthalene (DMN) unit, across 4–, 6–, and 8–bond bridges. However, measurements of V^*, for photoinduced charge separation in the neutral **DMN[*n*]DCV** compounds by Oevering *et al.* [13] gave much smaller values, which are much more in line with results obtained for other systems (see Table 5.5 and Figure 5.6). In the context of the Penfield *et al.* experiment, it should be noted that the radical-anion of the DCV group is prone to distort by twisting about the C=C double bond, thereby concentrating the unpaired electron on the carbon atom of the vinyl group that is attached to the bridge. This may well enhance the magnitude of the electronic coupling, V, in the anion radicals of these systems and it is, therefore, even more striking that with the very diffuse C_{60} acceptor, such strong coupling in **C_{60}[11]DMA** is achieved.

Table 5.5. *Experimental values for the electronic coupling matrix element $V^{(*)}$ for excited state (V) or thermal (V^*) electron transfer processes between electron donor and acceptor sites connected by extended arrays of n sigma bonds.*

Structure	*n*	$V^{(*)}$ (cm^{-1})
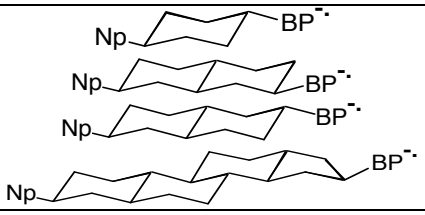	5 6 7 10	128[a] 54[a] 30[a] 6.2[a]
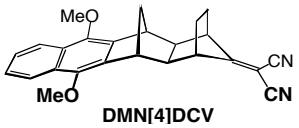 **DMN[4]DCV**	4	370[b]; 1300[c]
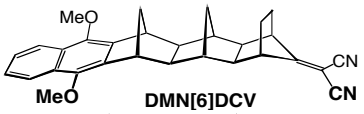 **DMN[6]DCV**	6	112[b]; 484[c]
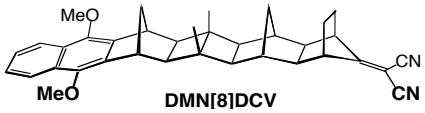 **DMN[8]DCV**	8	40[b]; 242[c]
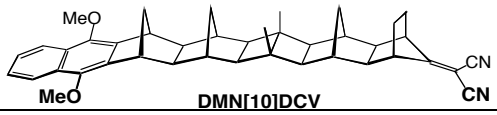 **DMN[10]DCV**	10	17.6[b]; --
	4	138[d]
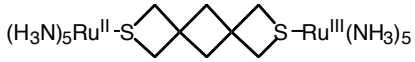	6	55[d]
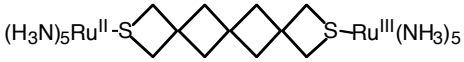	8	24[d]

a) From the rate of electron transfer of an anion radical centered on the BP (biphenyl) to the naphthalene (Np) unit [Closs and Miller 1988] [25]

b) From the radiative rate constant of charge transfer fluorescence [Oevering et al. 1989] [26]

c) From the inter valence absorption bands of the anion radical centered on the dicyanovinyl group [Penfield et al. 1987] [27]

d) From the inter valence absorption [Stein et al. 1982] [28]

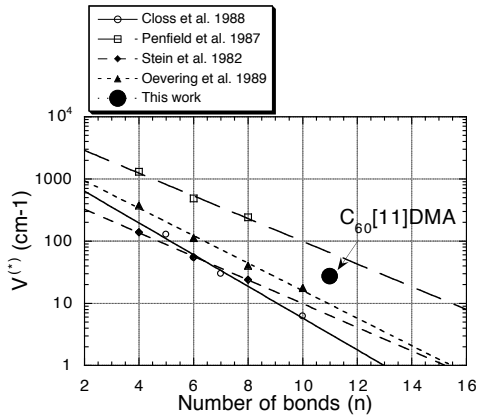

Fig. 5.6. *Semilogarithmic plot of various data sets from Table 5.5, showing the approximate exponential decay of $V^{(*)}$ with bridge length (n) and the extraordinary large value of V^* for the* **C_{60}[11]DMA** *system.*

We tentatively propose that the large V^* for **C_{60}[11]DMA** is mainly related to the special orbital symmetry properties of the fullerene π–system. Preliminary semi-empirical MO calculations are presented in the next section which lend support to this view.

5.5 Molecular orbital calculations

A simple frontier molecular orbital (FMO) description of photoinduced electron transfer in a D/A system, in which the acceptor has the lowest excited state is given in Figure 5.7.

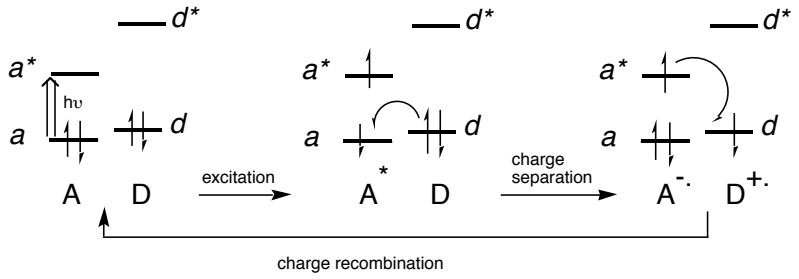

Fig. 5.7. *FMO representation of charge separation and charge recombination following local excitation of the acceptor in a D/A system.*